XIX IMEKO World Congress
Fundamental and Applied Metrology
September 6–11, 2009, Lisbon, Portugal

AN APPLICATION OF THE TCRBF NEURAL NETWORK IN MULTI-NODE FAULT DIAGNOSIS METHOD

Zbigniew Czaja [1], *Michał Kowalewski* [2]

[1] Gdansk University of Technology, Faculty of Electronics, Telecommunications and Informatics, Department of Optoelectronics and Electronic Systems, Gdansk, Poland, zbczaja@pg.gda.pl
[2] Gdansk University of Technology, Faculty of Electronics, Telecommunications and Informatics, Department of Optoelectronics and Electronic Systems, Gdansk, Poland, Michal.Kowalewski@eti.pg.gda.pl

Abstract – This paper presents the new self-testing method for diagnosis of analog parts in mixed-signal embedded systems controlled by microcontrollers. The tested analog part is stimulated by a sinus-wave supplied by the onboard generator and its responses are sampled in selected nodes by microcontrollers ADC. The measurement space is represented by differences between values of selected node voltages. Fault detection and localization is performed by a Two-Center Radial Basis Function (TCRBF) Neural Network. The diagnosis procedure was implemented and simulated in a PC.

Keywords fault diagnosis, neural network, BIST

1. INTRODUCTION

At present, embedded electronic systems which are characterized by an "intelligent unit", often based on a microcontroller, a digital signal processor (DSP) or a programmable device (e.g. FPGA, CPLD), predominate on the electronic market, because information about the operational environment and controlled objects are often obtained via analog sensors. Analog signals are transmitted and initially processed in analog parts, however analog-to-digital processing and data processing are realized by digital parts. Therefore, the analog part has to work correctly, because an incorrect measurement signal can lead to a wrong decision of the control unit, what can even result in damage of the controlled device. Hence, the embedded system should be able to run self-testing of analog parts.

Self-testing of analog circuits bases on fault diagnosis methods. When elaborating these methods we have to take into consideration continuous values of circuit elements, the continuous nature of stimulation and response signals and the fact that these signals can assume the shape of any function, the presence of element tolerances and circuit nonlinearities. Additionally, especially for non-electrical objects modelled by electrical circuits we have only poorly defined system models. Thus neural networks can be a very efficient solution in fault diagnosis methods. Many types of neural networks are used as fault classifiers: back-propagation [1], probabilistic [2], self-organizing [3] radial basis function [4,5], neural networks based on TCRB Functions [6].

In this paper a new self-testing procedure will be presented. It bases on a new multi-port fault diagnosis method and the simplified TCRBF neural classifier [7].

The diagnosis method is used to create a fault dictionary in the form of dispersed localization curves ideally suited for the TCRBF neural classifier. Additionally, measurements of parameters of the tested analog part are performed by the reconfigurable BIST created from peripheral devices of the control unit controlling the electronic embedded system.

2. FAULT DIAGNOSIS METHOD

The method will be illustrated on an exemplary analog part represented by the low-pass Tow-Tomas filter shown in Fig. 1.

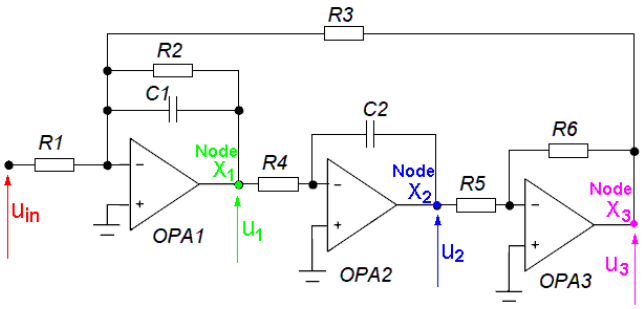

Fig. 1. Tested analog circuit – low-pass Tow-Tomas filter, where R1 = R2 = R3 = R4 = R5 = R6 = 10 kΩ, C1 = 33 nF, C2 = 6.8 nF

Generally, the self-testing procedure consists of three stages. At first, during the pre-testing stage, the TCRBF neural classifier is constructed on the basis of a family of dispersed localization curves. These curves describe the behaviour of the tested circuit following changes of its elements values. The second stage is responsible for sinus-wave stimulation of the tested circuit and for measurements of real and imaginary values of voltages in accessible nodes. At the last stage, the TCRBF neural classifier detects and localizes a fault of the analog part.

2.1. Idea of the method

Let $\boldsymbol{X}_N$ be a set of N accessible measurement nodes $\boldsymbol{X}_N = \{X_1, X_2, ..., X_N\}$. Thus, we have the following set of values of node voltages: $\boldsymbol{u}_N = \{v_n, w_n\}_{n = 1, ..., N}$, where

$u_n = v_n + j \cdot w_n$. These voltages can directly create a $(2 \cdot N)$-dimensional measurement space in a way similar to [9,10], but in this case localization curves representing deviations of values of circuit elements often characterize widely different lengths, which depends on circuit sensitivity, and often they are not situated optimally. This makes it difficult to perform correct fault localization.

Hence, it is proposed to create a new measurement space, where coordinates have the following forms: $\{v_{n,n-1}, w_{n,n-1}\}_{n=2,\ldots,N}$, where $v_{n,n-1}, = v_n - v_{n-1}$, $w_{n,n-1}, = w_n - w_{n-1}$. That is we create the space represented by differences between values of node voltages. In this case we improve the "dynamics" of length changes of localization curves. Lengths are more similar between themselves and curves are more separated as shown in Fig. 2 and Fig. 3.

It will be explained on the example of the circuit shown in Fig. 1. The denominator for all its node transfer functions is following:

$$d = R_1 \cdot (R_2 \cdot R_3 \cdot R_4 \cdot R_5 - X_2 \cdot R_3 \cdot R_4 \cdot R_5 + X_1 \cdot X_2 \cdot R_2 \cdot R_6) \quad (1)$$

where $X_1 = -1/(j\omega C_1)$, $X_2 = -1/(j\omega C_2)$. It is dependent on all elements, especially on R_1. However, the numerators for next node transfer functions have the forms:

$$\begin{aligned} m_1 &= X_1 \cdot R_2 \cdot R_3 \cdot R_4 \cdot R_5 \\ m_2 &= X_1 \cdot X_2 \cdot R_2 \cdot R_3 \cdot R_5 \\ m_3 &= -X_1 \cdot X_2 \cdot R_2 \cdot R_3 \cdot R_6 \end{aligned} \quad (2)$$

Thus, we obtain the following differences between numerators of transfer functions for respective nodes:

$$\begin{aligned} m_2 - m_1 &= X_1 \cdot R_2 \cdot R_3 \cdot R_5 \cdot (X_2 - R_5) \\ m_3 - m_2 &= X_1 \cdot X_2 \cdot R_2 \cdot R_3 \cdot (R_5 + R_6) \end{aligned} \quad (3)$$

It is seen from (2) and (3) that the difference $m_2 - m_1$ between the 1st and the 2nd node function numerators is dependent on the same elements as the respective numerators. The same situation is for the $m_3 - m_2$ difference. That is we decrease the size of the measurement space what decreases the size of the fault dictionary, simultaneously keeping the same level of the localization resolution. But this operation increases the "dynamic" of measurement signals, because signals for neighbouring nodes are moved about 180° and they added to themselves (see Fig. 1).

The new measurement space is described by the following transformation:

$$\begin{aligned} T_i(p_i) = \sum_{n=2}^{N} & \left(\mathrm{Re}\left(u_n(p_i) - u_{n-1}(p_i)\right)\mathbf{i}_{2n-2} \right. \\ & \left. + \mathrm{Im}\left(u_n(p_i) - u_{n-1}(p_i)\right)\mathbf{i}_{2n-3} \right) \end{aligned} \quad (4)$$

where: $\mathbf{i}_n$ - is a coordinate vector along the n axis, $u_n(p_i)$ – complex value of voltage in the node n for a change of p_i value of the i-th element, $i = 1,\ldots, I$, I – the number of circuit elements, N – the number of accessible measurement nodes.

The transformation (4) maps the changes of circuit element values $\{p_i\}_{i=1,\ldots,I}$ into a family of localization curves placed in the $(2 \cdot N - 2)$-dimensional measurement space. For the circuit shown in Fig. 1 we have a 4-dimensional space. Thus the transformation (1) is presented in two three-dimensional spaces (Fig. 2, 3). Localization curves in these figures were drawn for ±50% changes of element values with reference to their nominal values $p_{j\,nom}$.

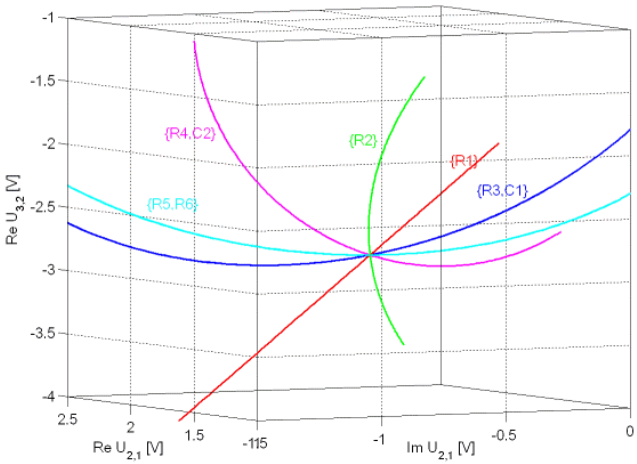

Fig. 2. The map of localization curves for the tested circuit in the 3-dimensional measurement space: Re($u_{2,1}$), Im($u_{2,1}$), Re($u_{3,2}$).

Localization curves are a graphical description of circuit proprieties following from changes of its element values. All curves cross at a point which is the nominal state of the circuit. Assumption of element tolerances causes dispersion of localization curves. Thus we need a classifier with good generalization capabilities to correctly localize faults. This requirement can be fulfilled by the TCRBF classifier, which is constructed on the basis of dispersed localization curves.

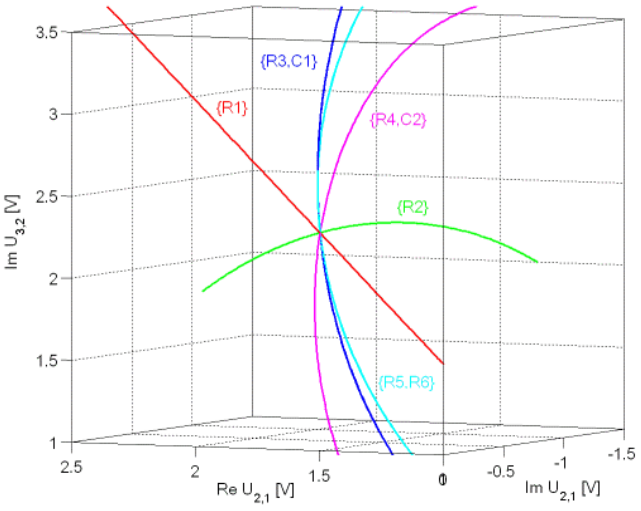

Fig. 3. The map of localization curves for the tested circuit in the 3-dimensional measurement space: Re($u_{2,1}$), Im($u_{2,1}$), Im($u_{3,2}$).

2.2. The measurement procedure

The measurement procedure is performed by microcontroller ATmega16 and its internal devices [11]: analog multiplexer, 10-bit ADC and 16-bit Timer 1 (Fig. 4).

The tested analog part is stimulated by the sinus-wave and its responses are sampled in particular nodes by the ADC in moments established by the Timer.

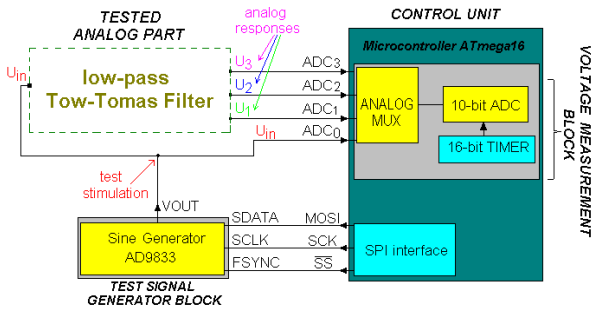

Fig. 4. Example of the electronic embedded system in the self-testing configuration

Timings of the measurement procedure are shown in Fig. 5. Each signal is sampled three times, where time distances between samples are set to one fourth of the period T. Time distances between samples for subsequent signals are equal to a half of the period. Thanks to this, it is allowed to sample all signals at the same moments in relation to the start of sampling, because sampling of the next signal is shifted about one period. Sampling of the input signal u_{in} is needed to establish a random shift time T_α of the sampling series. The third sample of each signal is used to eliminate the voltage offset. The first $u_{n,1}$ and second $u_{n,2}$ samples of the node voltage signal u_n are used to calculate their real and imaginary values.

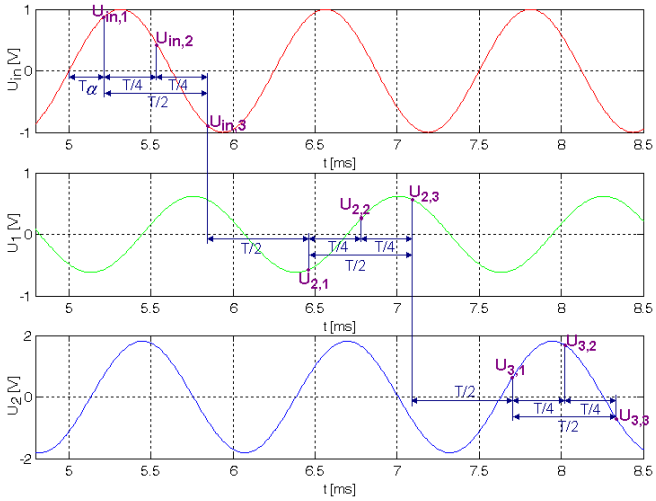

Fig. 5. Timings of the measured signals during the self-testing procedure in the input node and nodes X_1 and X_2.

The algorithm of the measurement procedure (Fig. 6) consists of a measurement part which is responsible for control of the measurement. The main function configures the ADC, starts the timer and waits for the end of sampling (it waits for the measurement of nine voltage samples). The interrupt service of the timer starts the ADC conversion and actualizes the counting time between next samples. The interrupt service of the ADC conversion complete saves the voltage samples and changes the channel of the analog multiplexer to measure the next node voltage. During the calculation part, the microcontroller computes the real v_n and imaginary w_n parts of the n-th node voltage basing on:

$$\begin{cases} v_n = \left(u_{n,1}\cdot u_{in,1} + u_{n,2}\cdot u_{in,2}\right)\cdot \chi \\ w_n = \left(u_{n,1}\cdot u_{in,2} - u_{n,2}\cdot u_{in,1}\right)\cdot \chi \end{cases} \tag{5}$$

where the value $\chi = 1 / U_{\text{in}}$ is constant and known, what considerably simplifies calculations of these values, because we use only addition and multiplication operations.

Next it calculates differences between these values: $v_{n,n-1}$, $= v_n - v_{n-1}$, $w_{n,n-1}$, $= w_n - w_{n-1}$.

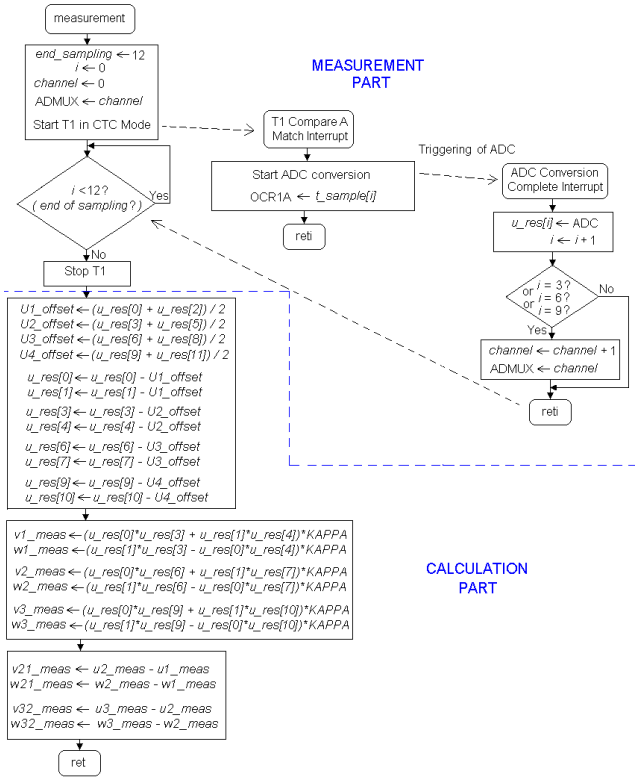

Fig. 6. The algorithm of the measurement procedure

3. USE OF THE TCRBF NEURAL NETWORK

Detection and localization of faults in the proposed method are performed by a neural network with TCRB functions [6,7]. The usefulness of the TCRB function in dictionary methods based on localization curves follows from the fact that the localization curve (Fig. 7a) can be transformed only with a few TCRB functions (Fig. 7d). In advance, some experiments with Radial Basis Function Neural Networks (RBFNN) for diagnosis purposes were performed [4,5]. Unfortunately an accurate transformation of localization curves with RBFNN requires a lot of Radial Basis (RB) functions in the architecture (Fig. 7b). Hence it appears an idea to construct a new neuron for better transformation of stretched clusters of dispersed localization curves.

The TCRB function radially maps the space around a line segment with endpoints $\mathbf{c}^{(1)}$ and $\mathbf{c}^{(2)}$ (Fig. 7c) with the following equation:

$$y(\mathbf{x}) = \exp\left(-\frac{1}{s^2(\mathbf{x})}\sum_{i=1}^{n}\left(x_i - w_i(\mathbf{x})\right)^2\right), \tag{6}$$

where: $s(\mathbf{x})$ is the *scaling function* describing the localization curve dispersion changing form σ_1 to σ_2 and $w_i(\mathbf{x})$ (i = 1, 2, …, n) are *center functions* depending on coordinates of centers $\mathbf{c}^{(1)}$ and $\mathbf{c}^{(2)}$ [6].

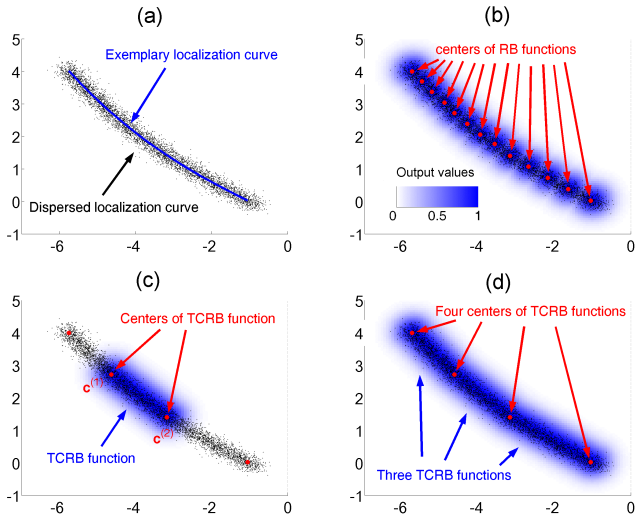

Fig. 7. Idea of localization curve transformation with RB and TCRB functions.

Applying some TCRB functions to each localization curve of the testing circuit gives the possibility to obtain information about distances between the measurement point and localization curves. This information is given as a vector of real values from the range (0, 1]. If the measurement point lies near the localization curve then one of TCRB functions assigned to that curve has the value close to 1. Otherwise, if the measurement point lies far from the localization curve, all TCRB functions assigned to this curve have values close to 0. The number of required TCRB functions for each localization curve depends on its curvature. For a curve similar to a straight line only one TCRBF is needed. The more bent the curve is the more TCRB functions are required. A graphical illustration of activation regions of TCRB functions for exemplary dispersed localization curves is shown in Fig. 8.

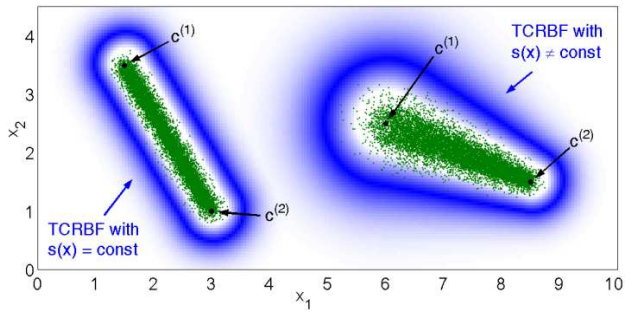

Fig. 8. Graphical illustration of activation regions of TCRB functions for exemplary dispersed localization curves.

3.1. Architecture of TCRBF classifier

The TCRBF classifier proposed in this paper is a three-layer feed-forward network (Fig. 9).

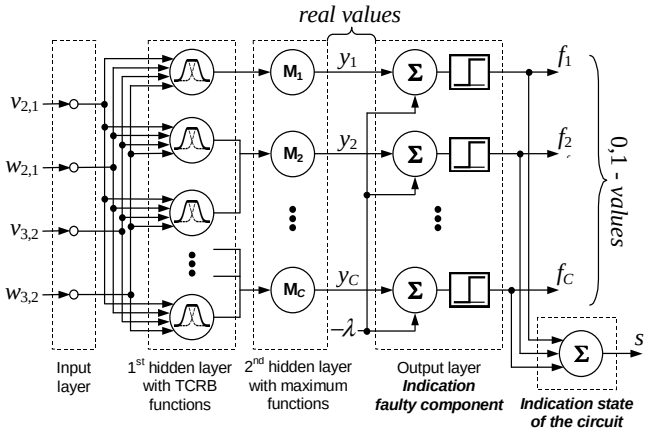

Fig. 9. The TCRBF neural network structure.

Its architecture is based on other neural networks with RB functions (RBFNN, Probabilistic, Generalised Regression). TCRB functions assigned to localization curves are placed in the 1st hidden layer. They play the role of radial mapping of dispersed localization curves to real values from the range (0, 1]. Dispersion is caused by circuit element tolerances. Neurons in the 2nd hidden layer group TCRB functions in C classes, which include singletons and ambiguity groups, and produce maximum values (M) of TCRBF outputs.

The output layer is a perceptron with a hard limit transfer function, which produces a vector $\boldsymbol{f}$ with 0 and 1 values. Each neuron in the output layer is fed only with two signals: maximum value of TCRB functions assigned to a class and constant bias $-\lambda$. The network output vector $\boldsymbol{f}$ combines information about the state of the testing circuit and moreover about the fault class.

An additional summing function sums perceptron output values and gives the value $s = f_1 + f_2 + \ldots + f_C$, which presents the state of the testing circuit as a single integer value from the range $[0, C]$.

The TCRBF classifier is able to distinguish between three states of the circuit: fault-free state ($s = C$), single fault or ambiguity group ($1 \le s < C$), multiple fault ($s = 0$).

A. Fault free state

If the measurement point is located near the nominal point then all TCRB functions located closest to the nominal point and assigned to different classes have output values $y_1, \ldots, y_C$ greater than λ. Hence the sum of all values from the perceptron outputs gives $s = C$. It indicates a fault-free state of the circuit.

B. Single fault or ambiguity group

Else if the measurement point is located near one of localization curves assigned to a fault class and far from others, then only one value y_i is grater than λ and the sum of all values from the perceptron outputs gives $s = 1$. In this case a single "one" in the output vector $\boldsymbol{f}$ indicates a fault class (single fault or ambiguity group). We meet with ambiguity also when $1 < s < C$. In this case the measurement point is located near more than one localization curves assigned to different fault classes.

C. Multiple fault

Finally if the measurement point is located far from any of localization curves then all values y_i are lower than λ and the sum of all values from the perceptron outputs gives $s = 0$. In this case we meet with a multiple fault and it is impossible to indicate which element is faulty.

A constant parameter $\lambda \in (0, 1)$, applied to the perceptron layer, makes it possible to describe the sizes of decision regions in the measurement space. For λ close to 1 decision regions are narrowed to spaces located near localization curves. It is best suited for circuits with small element tolerances. Otherwise, if λ is close to 0, decision regions are wide and circuits with greater element tolerances can be correctly diagnosed.

3.2. Construction of TCRBF classifier

In contrast to RBF or feed-forward back-propagation (FFBP) neural networks, TCRBFNN does not require training. Centers of TCRB functions are placed on localization curves of the testing circuit with a known model. Scaling parameters of TCRB functions are obtained on the basis of Monte Carlo analysis in selected centers.

The center selection method bases on linear interpolation of localization curves. Starting from two centers placed on extreme points of the localization curve, in next steps points farthest to the interpolation curve are selected as new centers and also as new interpolation nodes. This procedure is repeated until the maximum distances between localization and interpolation curves are lower then the assumed distance d_{max}.

In the second step for all selected centers the Monte Carlo analysis is performed in order to obtain localization curves dispersion. With assumption of normal distribution of points in each cluster, standard deviations of multivariate normal distribution are estimated and used as scaling parameters of TCRB functions.

Fig. 10 presents interpolation curves and data clusters obtained from the Monte Carlo analysis with assumption of 3% element tolerances for the circuit shown in Fig. 1.

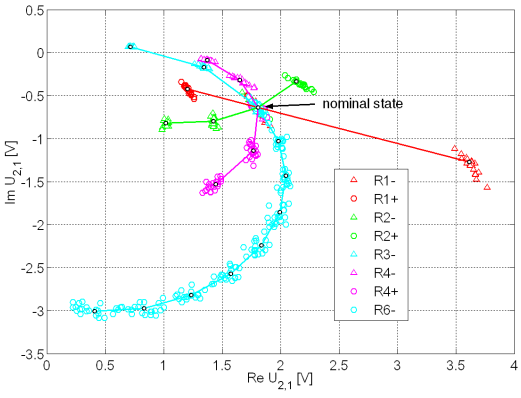

Fig. 10. Interpolation curves and data clusters obtained for the circuit shown in Fig. 1 and used in TCRBF classifier construction stage.

Connections between the 1st and the 2nd hidden layer are made easily, as we know the circuit model and know how to bind identification curves with fault classes. In case of lack of the circuit model, when only experimentally acquired measurements are available, TCRBF centers can be obtained with the fuzzy c-means clustering algorithm [4].

The parameter λ of the output layer is selected experimentally in order to decrease the classification error.

3.3. Simulation results

The proposed diagnosis procedure with the TCRBF classifier was used for faults detection and localization in the low-pass filter shown in Fig. 1. Three TCRBF classifiers with different architectures were constructed (Table 1) and their generalization capabilities were compared. A different number of the following input coordinates was used in each classifier: Re($u_{2,1}$), Im($u_{2,1}$), Re($u_{3,2}$), Im($u_{3,2}$).

Table 1. TCRBF classifiers parameters.

Input dimension	*Number of TCRB functions*	*Network architecture*	*Number of TCRB functions per each element*							
			R_1	R_2	R_3	R_4	R_5	R_6	C_1	C_2
2D	19	2-19-4-4	2	3	2	4	-	8	-	-
3D	28	3-28-5-5	2	3	7	5	3	8	-	-
4D	32	4-32-5-5	2	3	8	7	4	8	-	-

The number of TCRB functions and classes in each classifier depends on the dimension of the input space (except the curvature of localization curves). For more dimensions, localization curves are more distant from each other and faults are more distinguishable. In this case more TCRB functions are needed and more classes can be created.

Localization curves of some elements cover each other and form ambiguity groups, for example {R_4, C_2}. Hence one needs to apply TCRB functions only for one element in the ambiguity group. An increase in the number of input dimensions from 2 to 3 caused separation of localization curves in the ambiguity group {R_3, R_5, R_6, C_1}. For this group two classes were formed: {R_3,C_1} and {R_5, R_6}. Graphical illustrations of the 1st hidden layer (with TCRB functions) activation regions in 2- and 3-dimensional input spaces are shown in Fig. 11 and Fig. 12. We can see a very good fit to localization curves.

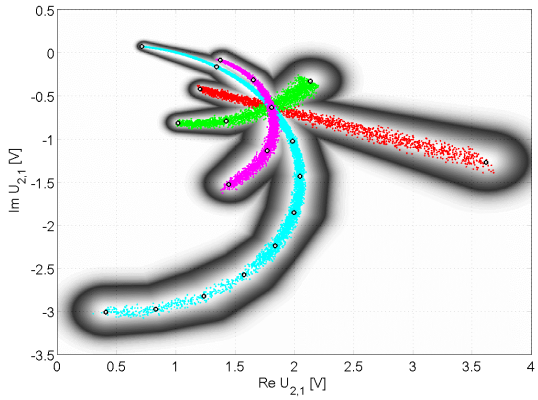

Fig. 11. Graphical transformation of dispersed localization curves by the TCRBF neural classifier in the 2-dimensional measurement space with coordinates: Re($u_{2,1}$), Im($u_{2,1}$).

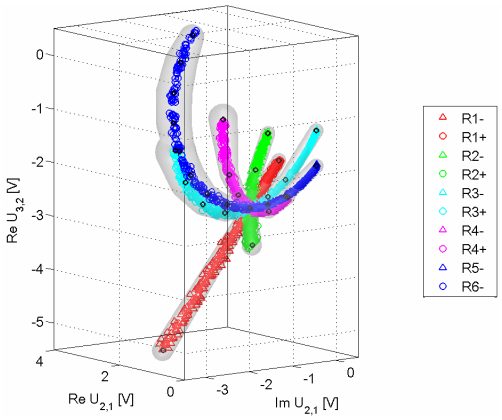

Fig. 12. Graphical transformation of dispersed localization curves by the TCRBF neural classifier in the 3-dimensional measurement space with coordinates: Re($u_{2,1}$), Im($u_{2,1}$), Re($u_{3,2}$).

The classification error of the created TCRBF classifiers did not exceed 2% and was mainly caused by improperly classified signatures near the nominal state of the circuit.

The TCRBF classifier constructed on a data set belonging to dispersed localization curves is able to distinguish between the nominal state of the circuit, single faults and multiple faults (Fig. 13). This feature can be achieved with the RBF neural network, but as mentioned earlier, a correct transformation of localization curves requires a significant increase in the number of RB functions.

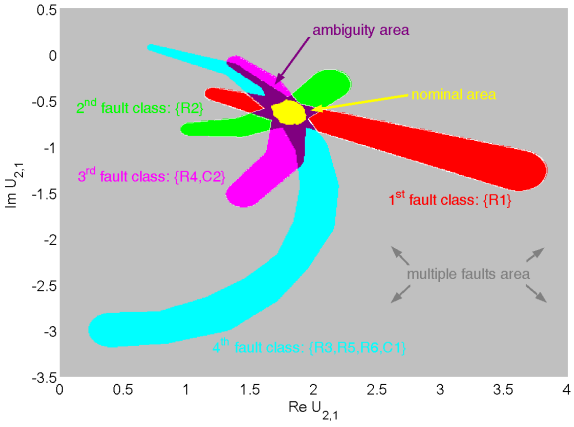

Fig. 13. Decision regions of the TCRBF classifier with the architecture 2 – 19 – 4 – 4 in the 2-dimensional measurement space for λ = 0.5.

In the case of the FFBP neural network with the architecture 3 – 30 – 5, trained on the same data set as the TCRBF classifier, the classification error on the test set exceeds 30%. It follows from the fact that neurons in FFBP network divide the pattern space using hyperplanes. Hence decision regions of that network go beyond dispersed localization curves and extend to infinity. To decrease this effect the FFBP network requires addition of a multiple faults data set in the training data set. Additionally the number of samples of the training set assigned to dispersed localization curves must be increased. This considerably extends the classifier construction procedure with reference to the TCRBF neural network.

4. CONCLUSIONS

The new self-testing method with the TCRBF classifier presented in this paper is an efficient way to diagnose analog parts in mixed-signal embedded systems controlled by microcontrollers. The novelty of the method lies in creating a new measurement space represented by differences between values of node voltages.

The TCRBF classifier used to detect the state of the circuit, as opposed to other types of neural classifiers (back-propagation, radial basis, probabilistic), has generalization capabilities ideally suited for dictionary methods based on localization curves. Unlike FFBP and RBF networks, the TCRBFNN requires a lower size of the data set used for construction. Hence the construction phase is shorter and less burdensome.

Furthermore, on the basis of the limited size of the construction data set, the TCRBF classifier gives the possibility to extend diagnostic information about the testing circuit. It is possible to distinguish between a fault-free state of the circuit, a single fault, an ambiguity group and a multiple fault.

REFERENCES

[1] Czaja Z., Zielonko R. “Fault diagnosis in electronic circuits based on bilinear transformation in 3-D and 4-D spaces”, *Trans. on Instr. and Measurement*, vol. 52, nº 1, pp. 97-102, 2003.

[2] Yang Z. R., Zwolinski M. “Applying a robust heteroscedastic probabilistic neural network to analog fault detection and classification”, *IEEE Trans. CAD IC&S*, vol. 19, pp. 142-151, 2000.

[3] Collins P., Yu S., Eckersall K. R., Jervis B. W., Bell I. M., Taylor G. E. “Application of Kohonen and supervised forced organization maps to fault diagnosis of electronic analog circuits”, *Electronic Letters*, vol. 30, nº 22, pp. 1846-1847, 1994.

[4] Catelani M., Fort A. ”Fault diagnosis of electronic analog circuits using a radial basis function network classifier”, *Measurement*, vol. 28, Issue 3, pp. 147-158, 2000.

[5] Toczek W., Kowalewski M. “A neural network based system for soft faults diagnosis in electronic circuits”, *Metrology and Measurements Systems*, vol. 12, nº 4, pp. 463-474, 2005.

[6] Kowalewski M. “Two-center radial basis function network for classification of soft faults in electronic analog circuits”, *In proc. of the IMTC’2007 Conference*, Warsaw, Poland, 2007.

[7] Czaja Z., Kowalewski M. “A new method for diagnosis of analog parts in electronic embedded systems with two center radial basis function neural networks”, *16th IMEKO TC4 Symposium*, pp. 743 - 748, Italy, Florence, September, 2008.

[8] Czaja Z., “A diagnosis method of analog parts of mixed-signal systems controlled by microcontrollers”, *Measurement*, vol. 40, nº 2, pp. 158-170, 2007.

[9] Czaja Z., “Using a square-wave signal for fault diagnosis of analog parts of mixed-signal electronic embedded systems”, *IEEE Transactions on Instrumentation and Measurement*, vol. 57, nº. 8, pp. 1589 – 1595, August, 2008.

[10] Czaja Z., “A fault diagnosis algorithm of analog circuits based on node-voltage relation”, *12th IMEKO TC1-TC7 Joint Symposium*, pp. 297 – 304, Annecy, France, September, 2008.

[11] Atmel Corporation, “8-bit AVR microcontroller with 16k Bytes In-System Programmable Flash, ATmega16, ATmega16L”, PDF file, *Available from: www.atmel.com*, 2003.